NACA

RESEARCH MEMORANDUM

A TRANSONIC WIND-TUNNEL INVESTIGATION OF THE EFFECTS OF BODY INDENTATION ON THE AERODYNAMIC CHARACTERISTICS OF AN APPROXIMATE-DELTA-WING—BODY CONFIGURATION, AND A COMPARISON WITH A WING OF REVERSED PLAN FORM

By Claude V. Williams

Langley Aeronautical Laboratory
Langley Field, Va.

NATIONAL ADVISORY COMMITTEE
FOR AERONAUTICS

WASHINGTON
August 13, 1953

NATIONAL ADVISORY COMMITTEE FOR AERONAUTICS

RESEARCH MEMORANDUM

A TRANSONIC WIND-TUNNEL INVESTIGATION OF THE EFFECTS OF BODY INDENTATION ON THE AERODYNAMIC CHARACTERISTICS OF AN APPROXIMATE-DELTA-WING—BODY CONFIGURATION, AND A COMPARISON WITH A WING OF REVERSED PLAN FORM

By Claude V. Williams

SUMMARY

Comparisons of the aerodynamic characteristics and a limited analysis of the flow phenomena as indicated by schlieren surveys for two approximate-delta-wing—body configurations have been made. The first of these configurations had a cylindrical afterbody while the afterbody of the second was indented in the region of the wing-body juncture so that the longitudinal distribution of the cross-sectional area normal to the axis of symmetry was the same as that for the cylindrical body alone.

Indentation resulted in relative decreases in the transonic drag-rise increments at moderate lift coefficients as well as at zero-lift conditions and also caused significant increases in the maximum lift-drag ratio at Mach numbers near 1.0. No major effect on the pitching-moment and center-of-pressure characteristics resulted from identation. The average lift-curve slope at Mach numbers near 1.0 was increased by indentation.

A comparison of the approximate-delta-wing—cylindrical-body configuration with a configuration having a highly tapered, unswept wing and a cylindrical body gave an indication of the effects of reversal of wing plan form on the aerodynamic characteristics of the configurations. This comparison indicated that plan-form reversal had little effect on the drag characteristics at Mach numbers near 1.0. Average lift-curve-slope values for the unswept-wing—cylindrical-body configuration were higher than those of the approximate-delta-wing—cylindrical-body configuration throughout the speed range. The location of the center of pressure of the approximate-delta-wing—cylindrical-body configuration was always more rearward than that of the unswept-wing—cylindrical-body configuration at all Mach numbers of this investigation.

INTRODUCTION

A new concept of the factors which influence the zero-lift transonic drag rise of wing-body configurations has been experimentally verified by the results of an investigation in the Langley 8-foot transonic tunnel. This concept, which was reported in reference 1, states that near the speed of sound the zero-lift drag rise of wing-body configurations with a thin, low-aspect-ratio wing is primarily a function of the longitudinal distribution of the cross-sectional areas normal to the axis of symmetry of the configurations.

Preliminary evaluations of the zero-lift drag-rise characteristics of an unswept, a swept, and an approximate-delta wing in combination with bodies modified on the basis of the drag-rise concept were also included in the tests of reference 1. The modified bodies had basically cylindrical afterbodies that were indented in the region of the wing-body juncture in a manner such that at any longitudinal station the cross-sectional area of the body of revolution was reduced by an amount equal to the cross-sectional area of the wing. Body indentation in this manner produced wing-body configurations which had longitudinal cross-sectional area distributions equivalent to the area distribution of the unindented cylindrical body alone. A comparison of the drag-rise characteristics of the indented configurations with the results obtained from tests of these wings in conjunction with the similar body that was unindented in the region of the wing-body juncture indicated that appreciable reductions of the zero-lift drag-rise increments associated with the wing resulted from body indentation (ref. 1). On the basis of the zero-lift results, further examinations of the characteristics of the wing-body configurations at moderate lift coefficients were made. The results of the expanded tests of the unswept-wing—body configurations and for the body alone are presented in reference 2, and the tests of the swept-wing—body configurations are reported in reference 3. The purpose of the present report is to present and analyze the results obtained from the extended investigations of the wing-body configurations with a wing of approximate-delta plan form.

A comparison is given herein of the aerodynamic characteristics of the cylindrical and indented configurations at moderate lift coefficients together with a brief analysis of the flow based on limited schlieren flow surveys. In addition, the present results for the approximate-delta-wing—cylindrical-body configuration are compared with the unswept-wing—cylindrical-body results of reference 2 to give an indication of the effects of reversal of wing plan form on the aerodynamic characteristics of the unindented-cylindrical-body configurations at transonic speeds. Since the rear portion of the body of the configurations of the present investigation does not approximate the contour and base size used on actual aircraft, the results presented cannot be used directly for the

design of such aircraft. However, it is believed that the relative effects of indentation and plan form as discussed in the report are indicative of those that would be obtained for an actual case.

SYMBOLS

C_D	drag coefficient adjusted to assumption of free-stream static pressure acting on model base, D/qS
C_L	lift coefficient, L/qS
C_m	pitching-moment coefficient about the 25-percent point of the wing mean aerodynamic chord, $\frac{M_{\bar{c}/4}}{qS\bar{c}}$
C_{D_o}	drag coefficient at zero lift
ΔC_{D_o}	incremental drag coefficient; the difference between the drag coefficient at a given Mach number and the arithmetical average of the drag coefficients at Mach numbers of 0.80 and 0.85
$\bar{c}$	wing mean aerodynamic chord
D	drag
L	lift
$M_{\bar{c}/4}$	pitching moment of aerodynamic forces about the 25-percent point of the wing mean aerodynamic chord
M	Mach number
q	dynamic pressure in undisturbed stream, $\frac{1}{2}\rho V^2$
S	wing area, includes wing area blanketed by body
V	velocity in undisturbed stream
α	angle of attack, deg
ρ	mass density in undisturbed stream

$\left(\frac{\partial C_L}{\partial \alpha}\right)_{av.}$ average lift-curve slope

$\left(\frac{L}{D}\right)_{max}$ maximum lift-drag ratio

APPARATUS

Tunnel

The investigation was conducted in the Langley 8-foot transonic tunnel (refs. 4 and 5). This facility has a dodecagonal, slotted test section in which the Mach number is continuously variable through the speed range up to a Mach number of approximately 1.13.

Models

Plan views and dimensional details of the sting-mounted models are presented in figure 1. The approximate-delta wing plan form of the present investigation was obtained by rotation of the unswept wing of reference 2 (shown herein as fig. 1(c)) about a spanwise axis so that the trailing edge of the unswept wing became the leading edge of the delta wing. This approximate-delta wing had an aspect ratio of 4, a taper ratio of 0, a sweepback of the quarter-chord line of 27.6°, and circular-arc airfoil sections parallel to the vertical plane of symmetry. The wing thickness ratio was 4 percent, and the point of maximum thickness was located at 60 percent of the chord.

One of the two approximate-delta-wing—body configurations, to be identified hereinafter as the "delta cylindrical configuration," had an afterbody that was cylindrical (fig. 1(a)). The other configuration, herein designated as the "delta indented configuration" (fig. 1(b)), differed from the first in that the body in the region of the wing-body juncture was indented so as to reduce the cross-sectional area of the body of revolution by an amount equal to the cross-sectional area of the wing at the same longitudinal station. Forebody dimensional coordinates are presented in table I. Dimensional coordinates of the indented afterbody are presented in table II. The unswept-wing—cylindrical-body configuration of reference 2 (fig. 1(c)) is to be identified herein as the "unswept cylindrical configuration."

The longitudinal distributions of the total cross-sectional areas normal to the axis of symmetry for the present configurations, and for the unswept cylindrical configuration are presented in figure 2.

The sting model support had approximately the same diameter as the rear portions of the body so as to reduce the effects of the model sting on the results; however, the diameter of the sting was somewhat less than that of the body to allow for deflections of the strain gage within the model.

TESTS AND MEASUREMENTS

Tests

The tests reported herein were made at Mach numbers of 0.80 to 1.10 and at angles of attack from 0° to 6°. The Reynolds number varied from 2.5×10^6 to 2.7×10^6 when based on the wing mean aerodynamic chord of 8 inches.

Force Measurements

The normal, axial, and pitching-moment characteristics of the models were measured by an internally mounted, electrical-strain-gage force balance. With this system the repeatability of lift coefficient was ± 0.004, and of pitching-moment coefficient was ± 0.003. Repeatability of the zero-lift drag coefficients was within ± 0.0005. At lifting conditions the drag coefficient repeatability was ± 0.001. It is believed that the several comparisons of the data herein are valid to approximately the same magnitudes.

The model angle of attack was measured by the fixed-pendulum, electrical-strain-gage system described in reference 2. The accuracy of this system is believed to be within $\pm 0.1^{\circ}$.

Static pressures near the model base were measured by orifices located in the sting approximately 1/4 inch forward of the plane of the model base. These measurements were used to adjust the drag coefficients to conform with the assumption of free-stream static pressure acting on the base of the model.

Due to the nature of the flow in the slotted test section, choking and blockage effects both for the zero-lift and for the moderate-lift cases presented are negligible and, therefore, no corrections were applied. The effects of wall-reflected disturbances on the drag results, as discussed in reference 5, have been practically eliminated at all Mach numbers except those near a value of 1.05 by offsetting the model from the tunnel center line, and by adjusting for base pressures. No data points are presented for a Mach number of 1.05, and no corrections for these boundary-reflected interference effects have been applied to the data;

however, the data when plotted against Mach number have been faired through this Mach number range since the comparative values are believed to be satisfactory.

Flow Measurements

The schlieren flow survey was made with the horizontally located, single-pass system described in reference 5.

The maximum random error in indicated stream Mach number is believed to be about 0.003. Mach number deviations in the region of the model generally increased with Mach number but did not exceed approximately 0.006 at stream Mach numbers up to 1.13 (ref. 5).

PRESENTATION OF RESULTS

The results of the investigation of the delta cylindrical (fig. 1(a)) and delta indented (fig. 1(b)) configurations are presented in the following figures:

	Figure
Basic aerodynamic characteristics	3
Zero-lift drag characteristics	4
Drag characteristics at lift coefficients of 0.2 and 0.4	5
Maximum lift-drag ratio and lift coefficients for maximum lift-drag ratio	6
Average lift-curve slopes	7
Center-of-pressure location	8
Flow phenomena at an angle of attack of 0°	9
Flow phenomena at an angle of attack of 4°	10

The effects of reversal of wing planform as given by a comparison of the data from reference 2 for the unswept-wing—cylindrical-body configuration (fig. 1(c)) with the data for the delta-cylindrical configuration of the present report is given in the following figures:

	Figure
Basic aerodynamic characteristics	11
Zero-lift drag characteristics	12
Drag characteristics at lift coefficients of 0.2 and 0.4	13
Maximum lift-drag ratios and lift coefficients for maximum lift-drag ratios	14

Figure

Average lift-curve slopes 15
Center-of-pressure locations 16

The drag characteristics for the delta cylindrical and delta indented configurations at zero-lift conditions as presented in reference 1 are repeated in figure 4 for convenience. The average lift-curve slopes $\left(\frac{\partial C_L}{\partial \alpha}\right)_{av.}$ presented in figure 7 were obtained from those lower portions of the curves of angle of attack plotted against lift-coefficient where approximate linearity existed. In general, departure from linearity occurred between 4° and 6° angle of attack.

Comparisons of the flow phenomena at angles of attack of 0° and 4° as seen from schlieren flow-field surveys are presented in figures 9 and 10, respectively. In these figures the left row of photographs (figs. 9(a) and 10(a)) shows the flow field about the delta cylindrical configuration, while the right row (figs. 9(b) and 10(b)) presents the flow about the delta indented configuration. Opposing photographs are for the same Mach number. The sketches of the models at the bottom of the figures are drawn to the same dimensional scale as that of the schlieren photographs. The photographs immediately above the model drawings are oriented in a manner so as to reproduce the relative locations of the model and flow survey field during the investigations.

DISCUSSION

Force Characteristics of Delta-Cylindrical and Delta-Indented Configurations

Drag at constant lift coefficient.- The zero-lift drag results have been discussed in reference 1 and are briefly reviewed herein. These results, presented in figure 4, indicate that at subsonic speeds the delta indented configuration had higher drag values than did the delta cylindrical configuration. This higher drag was probably the result of losses in the boundary layer associated with the local flow over the rearward end of the indentation. However, at Mach numbers above 0.93, indentation appreciably reduced the drag relative to that of the delta cylindrical configuration. This reduction was a maximum at a Mach number of approximately 1.0. At lift coefficients of 0.2 and 0.4, indentation generally reduced the value of the drag coefficient throughout the speed range of this investigation (fig. 5) and, as was the case for the zero-lift condition, the reduction of the drag was greatest near a Mach number of 1.0.

Maximum lift-drag ratio.- The results presented in figure 6 show that indentation increased the value of the maximum lift-drag ratio throughout the Mach number range of this investigation and the increases were appreciable throughout the Mach number range from 0.95 to 1.05 where the value of the maximum lift-drag ratio was increased approximately 20 percent.

Lift, pitching-moment, and center-of-pressure characteristics.- Reference to figures 3(a) and 7 indicates that the body indentation increased the lift-curve slope in the speed range near a Mach number of 1.0. The indentation generally had no major effect on the pitching-moment and center-of-pressure characteristics of the configurations investigated (figs. 3(c) and 8).

Flow Phenomena of Delta-Cylindrical and Delta-Indented Configurations

Angle of attack of 0°.- An examination of the schlieren photographs for the delta cylindrical configuration (fig. 9(a)) indicates the presence of a strong shock wave behind the trailing edge of the wing. This shock is associated with the deceleration or compression of the flow about the wing. The area distribution for the delta cylindrical configuration (fig. 2) shows the rather abrupt longitudinal variation of the cross-sectional area of the wing which is mainly responsible for the presence of the shock.

Comparisons of the photographs of the flow about the delta indented configuration (fig. 9(b)) with those of the delta cylindrical configuration indicate that indentation reduced the local Mach number of the flow in the region of the wing. This phenomenon is illustrated by a comparison of the radial extent of the shocks at a Mach number of 0.98, and by a comparison of the inclination angles and apparent strengths of the various shock waves at Mach numbers above 0.98. The most forward shock shown in the photographs for the delta indented configuration is believed to be associated with the curvature of the indentation as discussed in reference 2.

Since the zero-lift drag of any configuration at transonic speeds is primarily a direct function of the strength or energy losses through the shock-wave system about the configuration, and the energy loss is associated with the Mach number of the flow; then, it follows that the comparative reduction in the Mach number of the flow field about the wing which resulted from body indentation was responsible for the drag reductions measured in this investigation.

Angle of attack of 4°.- The schlieren investigation at an angle of attack of 4° was limited in that no observations of the flow in the region below the wing-body juncture were made, and therefore no quantitative comparisons can be made. However, an examination of the photographs of the flow in the region above the trailing edge of the wing-body juncture, presented in figure 10, indicates that especially for the delta indented configuration, a complex shock system existed about the juncture. The presence of this shock system indicates that the indentation designed for zero-lift conditions loses effectiveness at lifting conditions. It may be surmised that as for the zero-lift case the reduction of the Mach number of the flow in the region of the wing was primarily responsible for the observed reduction in drag for the delta indented configuration.

Effect of Reversing Wing

General comments.- An analysis of the effects of reversal of wing plan form is given by a comparison of the delta cylindrical configuration of the present paper with the unswept cylindrical configuration of reference 2. It should be pointed out that the plan form of the wing was not the only variable involved in the comparison. Rotation of the unswept wing about a spanwise axis changed the airfoil section thickness distribution and also the chordwise location of the maximum thickness. However, it is believed that these variables were of secondary importance, and hence that this comparison gives an evaluation of the effects of reversal of wing plan form.

Drag at constant lift coefficients.- The drag characteristics presented in figures 12 and 13 indicate that the major effects of reversing the plan form were evident below a Mach number of approximately 0.90. For the zero-lift case, the drag of the unswept cylindrical configuration was somewhat higher than that of the delta cylindrical configuration. Reference to the incremental-drag-coefficient curves indicates that the drag rise of the delta cylindrical configuration was higher than that of the unswept cylindrical configuration. On the basis of these and similar data, it was deduced in reference 1 that, near the speed of sound, a given rate of decrease in cross-sectional area generally results in a greater drag rise than a similar rate of increase.

Reference to figure 13 (drag characteristics at lift coefficients of 0.2 and 0.4) indicates that at Mach numbers less than 0.90, the unswept cylindrical configuration had considerably lower values of drag coefficient than did the delta cylindrical configuration. It is believed that these lower drag-coefficient values resulted from the smaller amount of flow separation at the leading edge of the unswept wing as compared with that for the approximate-delta wing which had greater sweep and a sharper leading edge. This belief is substantiated to some extent by the fact

that the lift-curve slope of the straight wing was higher than that for the delta wing. As the Mach number approached 0.90, the development of supersonic flow about the leading edge of the approximate-delta wing apparently reduced the amount of separation so that the drag became approximately the same as that for the unswept wing.

Maximum lift-drag ratio.- A comparison of the maximum-lift-drag-ratio characteristics (fig. 14) indicates that, because of the relatively higher drag values at lifting conditions for the delta cylindrical configuration, below a Mach number of approximately 0.90, the delta cylindrical configuration had somewhat lower values of the maximum lift-drag ratio than did the unswept cylindrical configuration. At Mach numbers above 0.90, the maximum-lift drag-ratio characteristics were the same.

Lift and pitching-moment characteristics.- Reference to figures 11(a) and 15 indicates that, throughout the Mach number range, the unswept cylindrical configuration had a higher lift-curve slope than did the delta cylindrical configuration. This fact agrees with the usual reduction in level of lift-curve slope associated with increase in sweep angle (ref. 6).

In figure 11(c) is presented a comparison of the pitching-moment variations for the two configurations. These data indicate that, throughout the Mach number range of this investigation at any particular Mach number, the slopes of the pitching-moment curves for the delta cylindrical configuration were always relatively more negative than those of the unswept cylindrical configuration. This characteristic is associated with the more rearward location of the center of pressure for the delta cylindrical configuration, figure 16. Throughout the Mach number range of this investigation, the center of pressure for the delta cylindrical configuration was approximately 10 percent rearward of that for the unswept cylindrical configuration.

CONCLUSIONS

The results of an investigation at Mach numbers of 0.80 to 1.10 of the effects of body indentation, as specified by the transonic drag-rise rule, of an approximate-delta-wing—body configuration led to the following conclusions:

1. The transonic drag-rise increments were reduced by indentation at moderate-lift as well as at zero-lift conditions, and the lift-curve slope was somewhat increased at Mach numbers above 0.95.

2. The reductions of the drag coefficients and the increase in lift-curve slope resulted in significant increases in the maximum lift-drag ratio at Mach numbers near 1.00.

3. Indentation had no major effect on the pitching-moment and center-of-pressure characteristics of the configurations investigated.

An analysis of the force characteristics of the delta cylindrical and unswept cylindrical configurations at Mach numbers from 0.80 to 1.10 led to the following conclusions:

1. The configurations had essentially the same drag characteristics at Mach numbers near 1.0 for the zero and moderate lift coefficients of this investigation.

2. Average lift-curve slopes for the delta cylindrical configuration were less than those of the unswept cylindrical configuration throughout the Mach number range.

3. Throughout the Mach number range the slopes of the pitching-moment curves for the delta cylindrical configuration were more negative than those of the unswept cylindrical configuration.

4. At moderate lift coefficients the center of pressure of the delta cylindrical configuration was approximately 10 percent rearward of that of the unswept cylindrical configuration at all Mach numbers of this investigation.

Langley Aeronautical Laboratory,
National Advisory Committee for Aeronautics,
Langley Field, Va., May 26, 1953.

REFERENCES

1. Whitcomb, Richard T.: A Study of the Zero-Lift Drag-Rise Characteristics of Wing-Body Combination Near the Speed of Sound. NACA RM L52H08, 1952.

2. Williams, Claude V.: A Transonic Wind-Tunnel Investigation of the Effects of Body Indentation, As Specified by the Transonic Drag-Rise Rule, on the Aerodynamic Characteristics and Flow Phenomena of an Unswept-Wing—Body Combination. NACA RM L52L23, 1953.

3. Robinson, Harold L.: A Transonic Wind-Tunnel Investigation of the Effects of Body Indentation, As Specified by the Transonic Drag-Rise Rule, on the Aerodynamic Characteristics and Flow Phenomena of a 45° Sweptback-Wing—Body Combination. NACA RM L52L12, 1953.

4. Wright, Ray H., and Ritchie, Virgil S.: Characteristics of a Transonic Test Section With Various Slot Shapes in the Langley 8-Foot High-Speed Tunnel. NACA RM L51H10, 1951.

5. Ritchie, Virgil S., and Pearson, Albin O.: Calibration of the Slotted Test Section of the Langley 8-Foot Transonic Tunnel and Preliminary Experimental Investigation of Boundary-Reflected Disturbances. NACA RM L51K14, 1952.

6. Luoma, Arvo A.: Aerodynamic Characteristics of Four Wings of Sweepback Angles 0°, 35°, 45°, and 60°, NACA 65A006 Airfoil Section, Aspect Ratio 4, and Taper Ratio 0.6 in Combination with a Fuselage at High Subsonic Mach Numbers and at a Mach Number of 1.2. NACA RM L51D13, 1951.

TABLE I.- ORDINATES OF FOREBODY

Distance measured from body nose, in.	Radius measured from body center line, in.
0	0
.225	.104
.338	.134
.563	.193
1.125	.325
2.250	.542
3.375	.726
4.500	.887
6.750	1.167
9.000	1.391
11.250	1.559
13.500	1.683
15.750	1.770
18.000	1.828
20.250	1.864
22.500	1.875

TABLE II.- ORDINATES OF INDENTED AFTERBODY

Distance measured from body nose, in.	Radius measured from body center line, in.
22.50	1.875
24.00	1.875
24.50	1.868
25.00	1.856
25.50	1.837
26.00	1.812
26.50	1.773
27.00	1.743
27.50	1.710
28.00	1.664
28.50	1.642
29.00	1.580
29.50	1.533
30.00	1.487
30.50	1.470
31.00	1.476
31.50	1.521
32.00	1.622
32.50	1.720
33.00	1.807
33.50	1.857
34.00	1.875
43.00	1.875

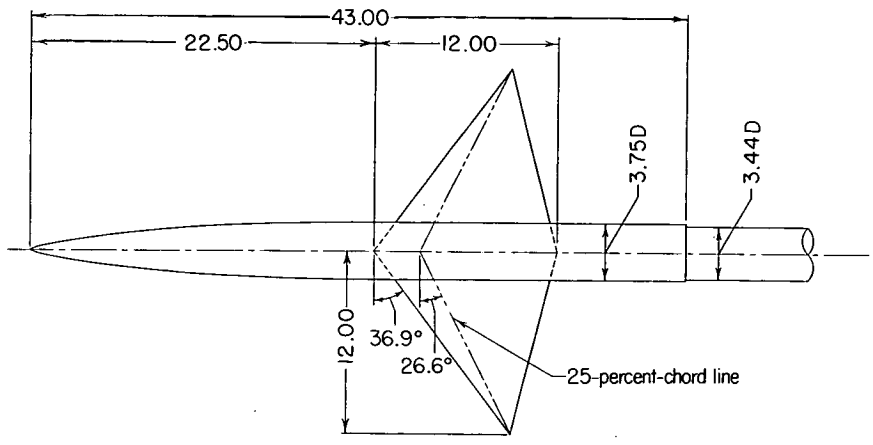

(a) Delta cylindrical configuration.

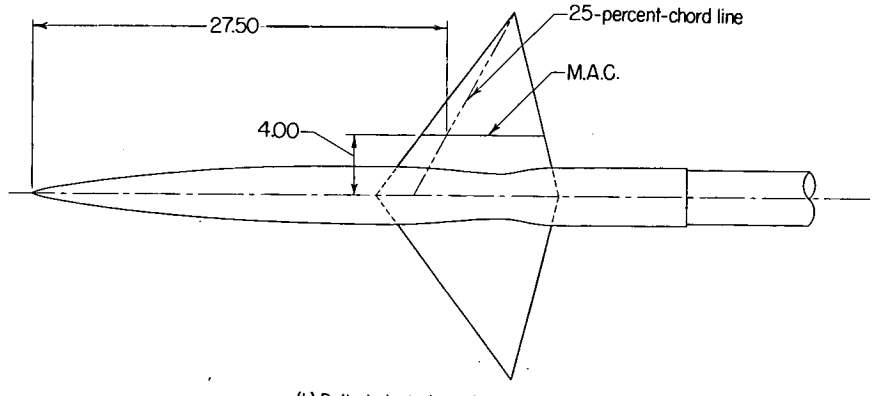

(b) Delta indented configuration.

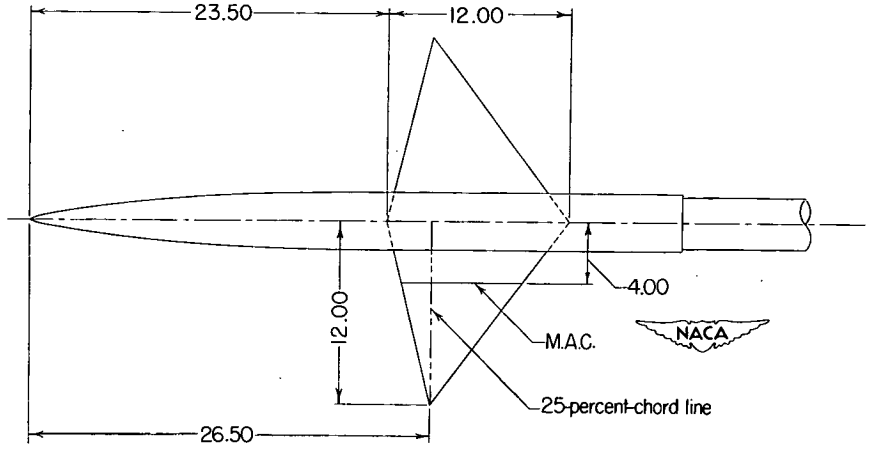

(c) Unswept cylindrical configuration. (Ref. 2).

Figure 1.- Plan views and dimensional details of the models investigated. All dimensions in inches.

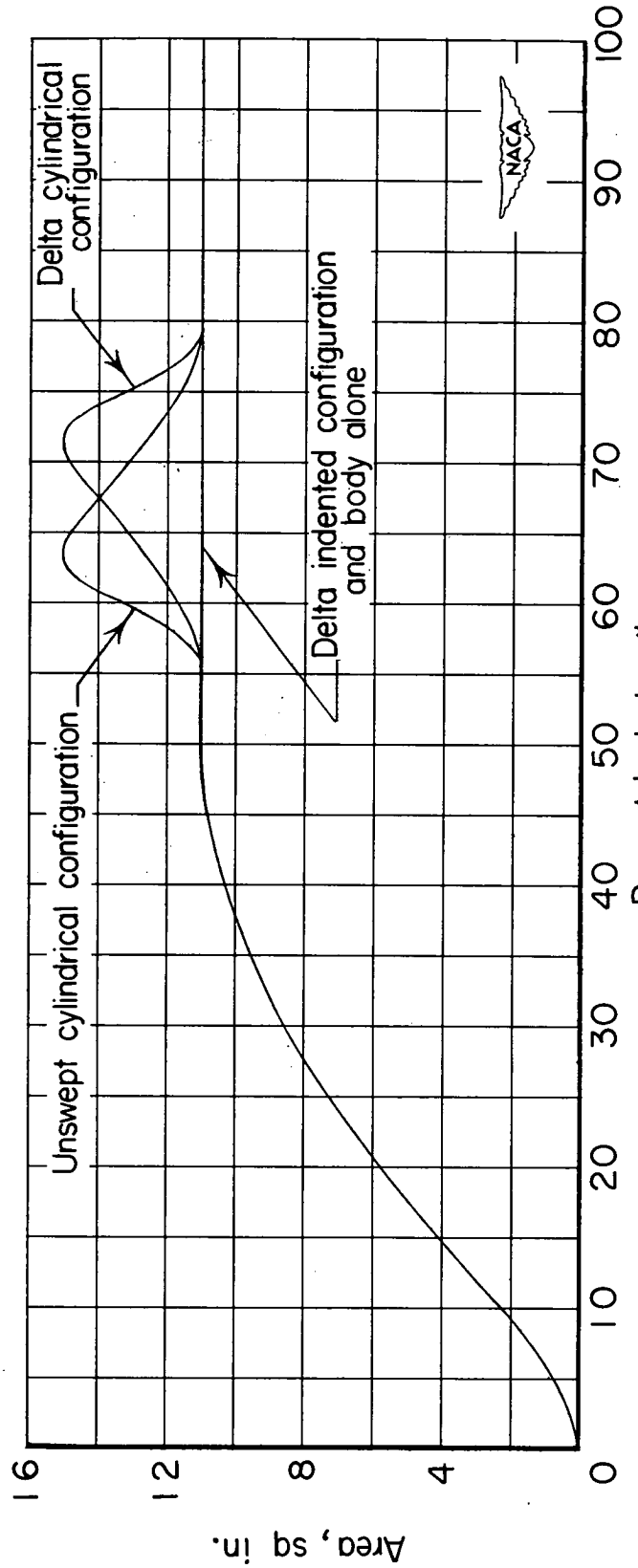

Figure 2.- Axial variation of the cross-sectional areas normal to the axis of symmetry for the models investigated.

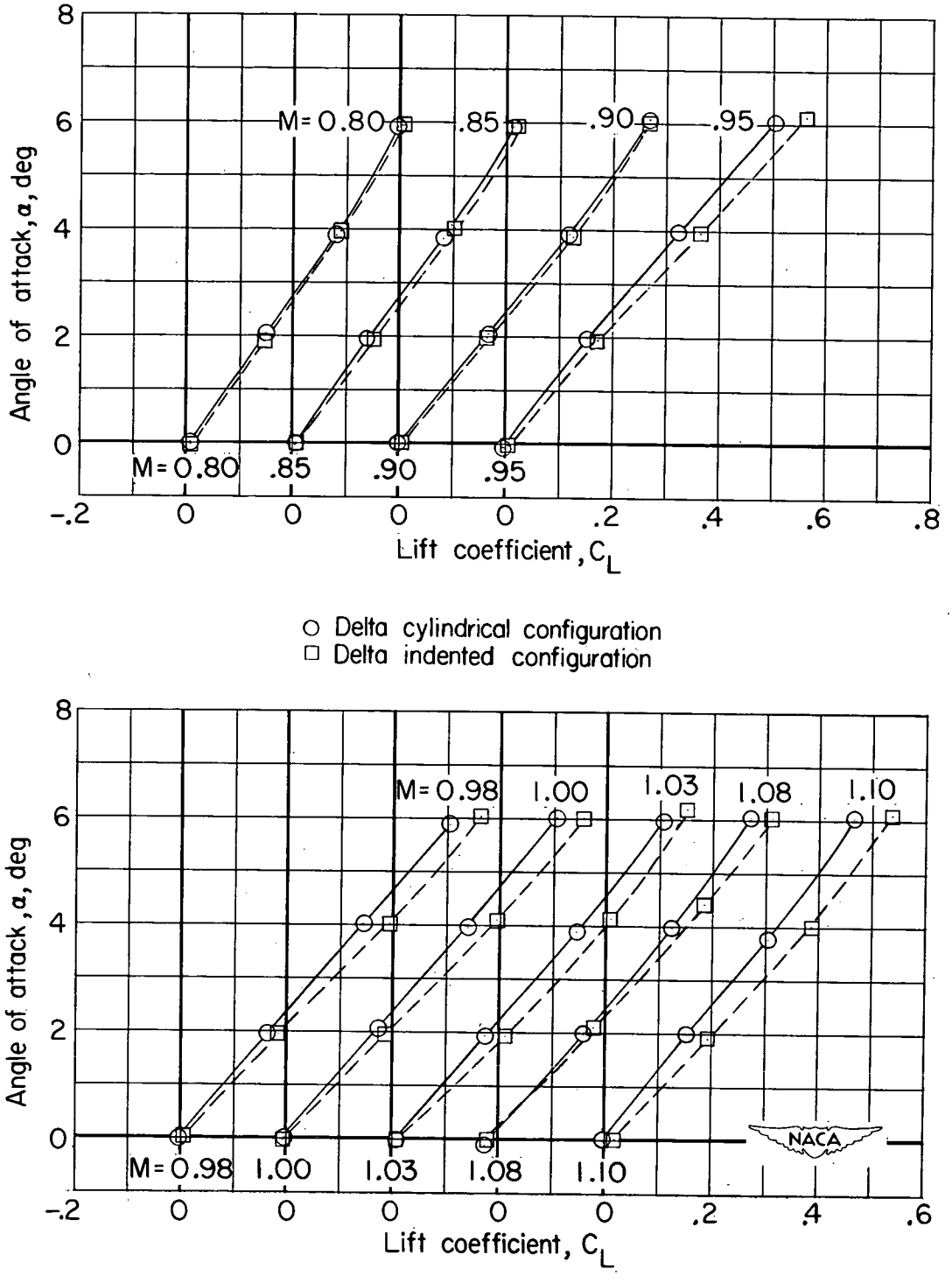

(a) α against C_L.

Figure 3.- Basic aerodynamic characteristics for the delta cylindrical and delta indented configurations at several Mach numbers.

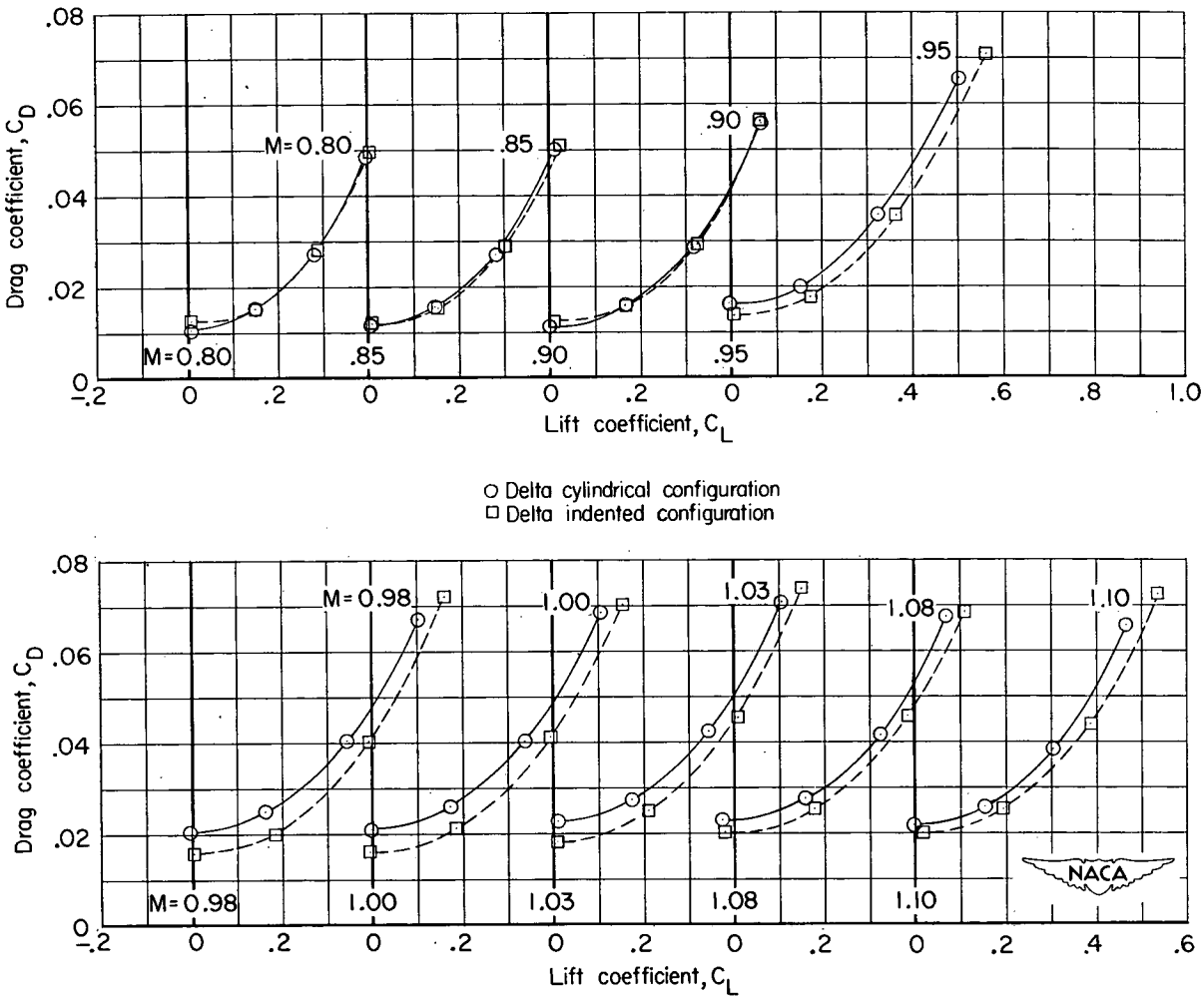

(b) C_D against C_L.

Figure 3.- Continued.

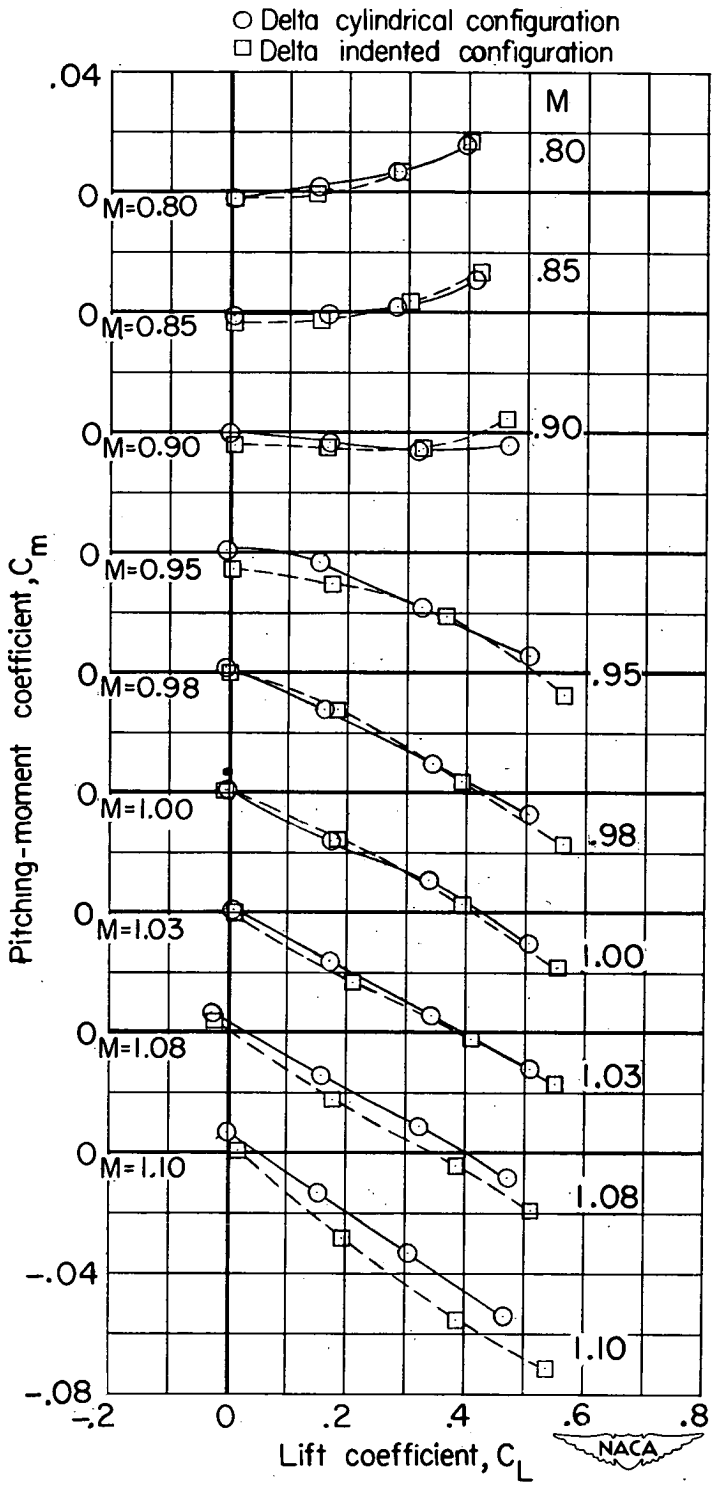

(c) C_m against C_L.

Figure 3.- Concluded.

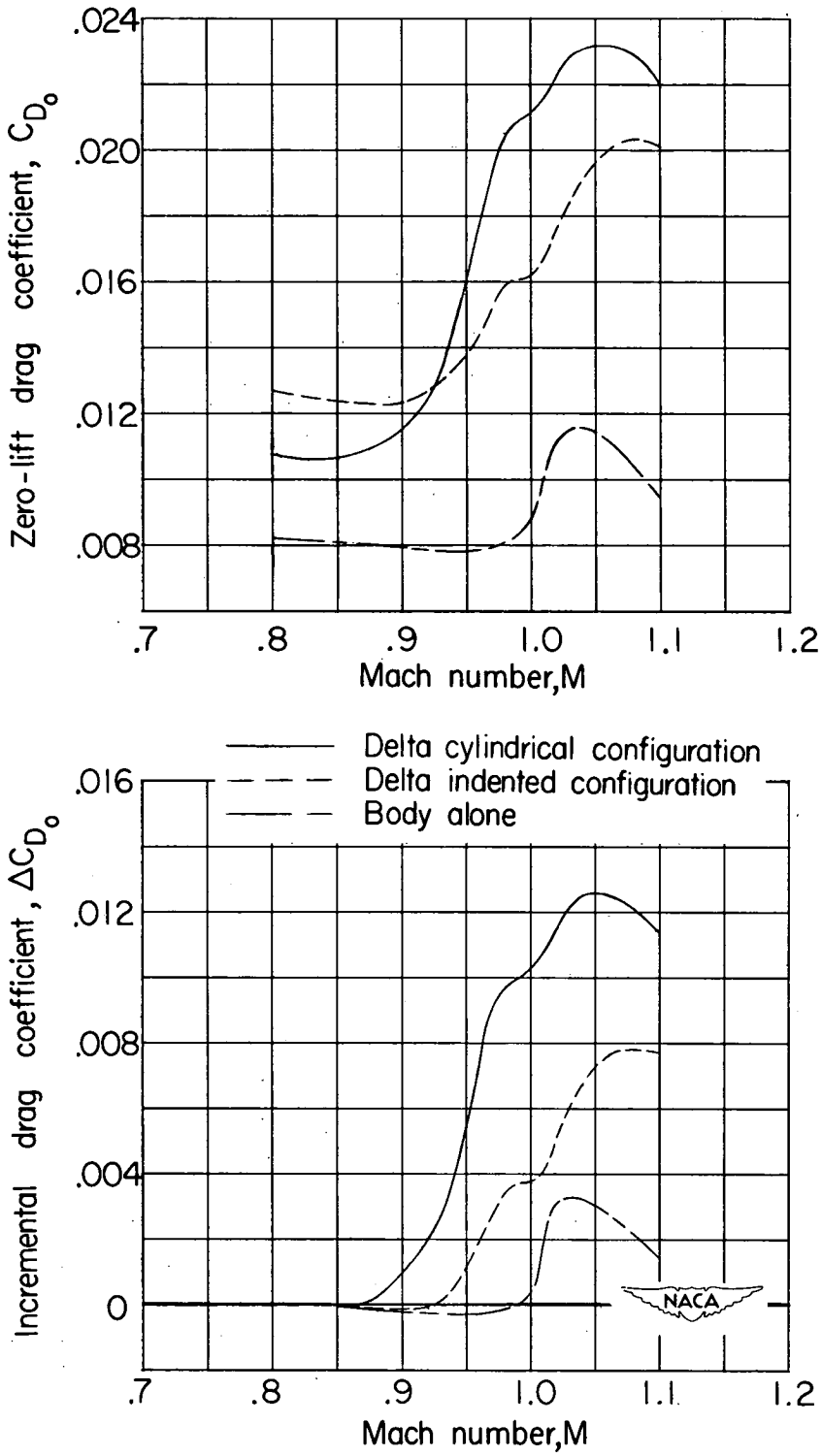

Figure 4.- Drag characteristics at zero lift for the delta cylindrical and delta indented configurations, and for the body alone. (Data from ref. 1.)

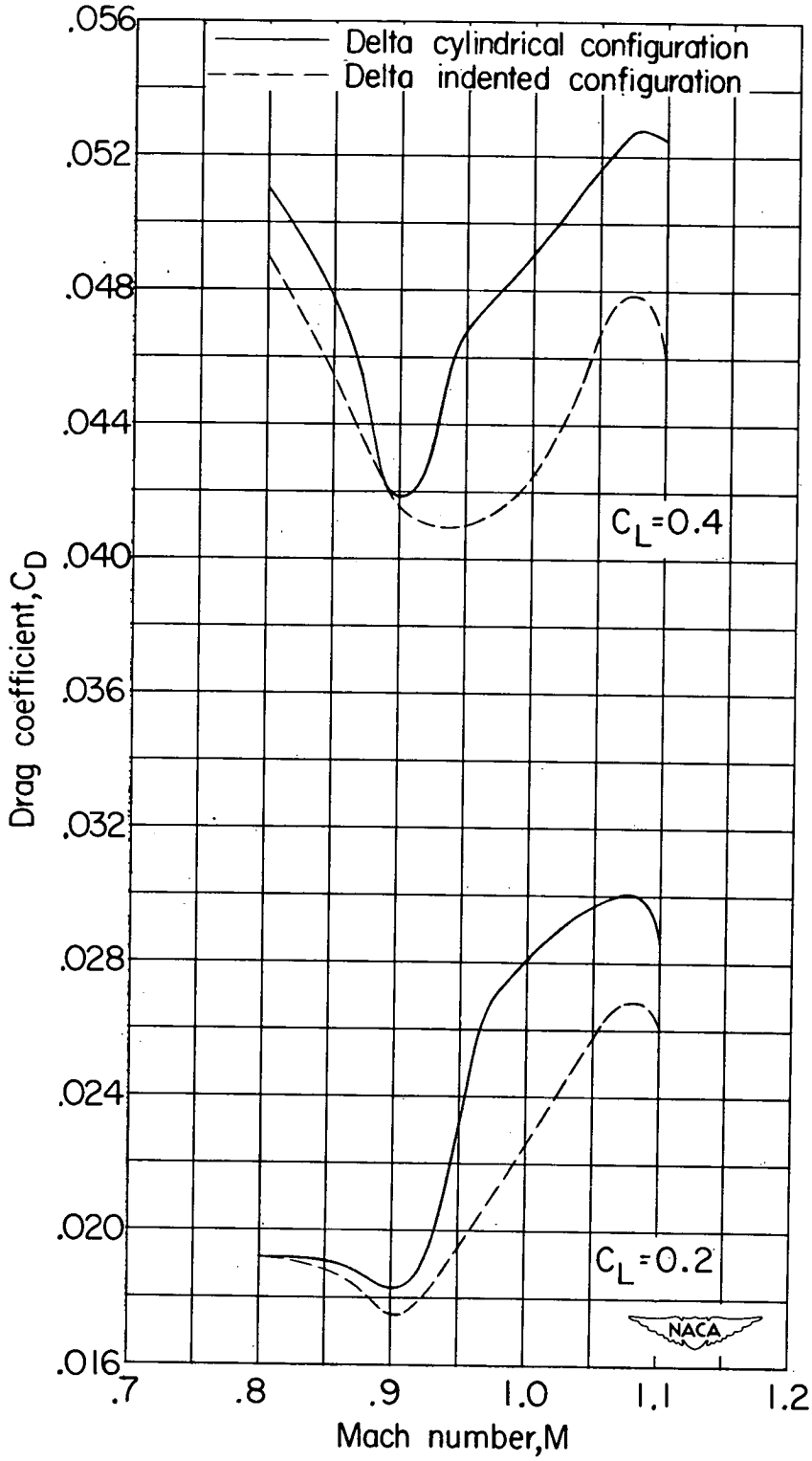

Figure 5.- Drag characteristics at lift coefficients of 0.2 and 0.4 for the delta cylindrical and delta indented configurations.

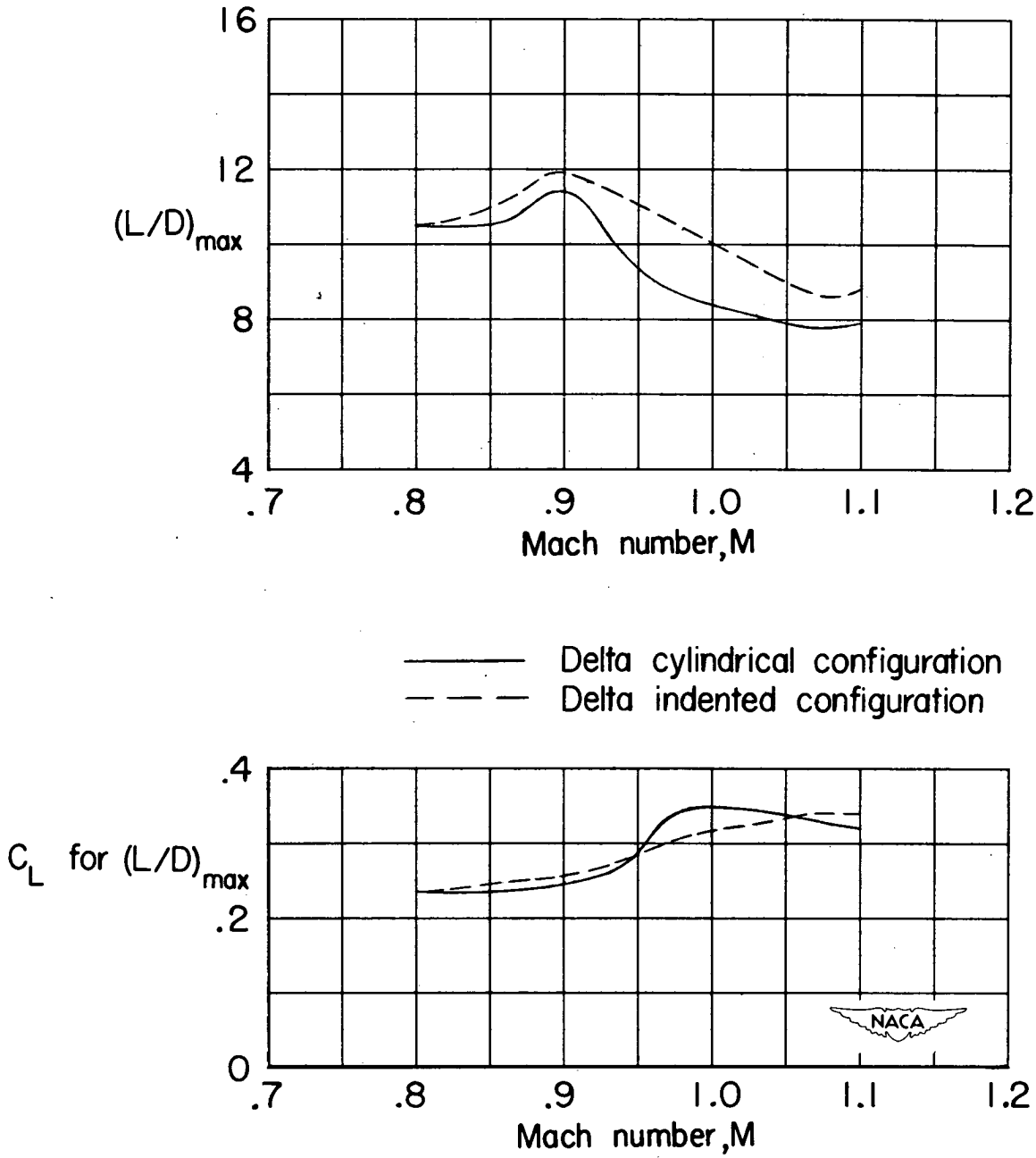

Figure 6.- Maximum lift-drag ratio, and lift coefficients for maximum lift-drag ratio for the delta cylindrical and delta indented configurations.

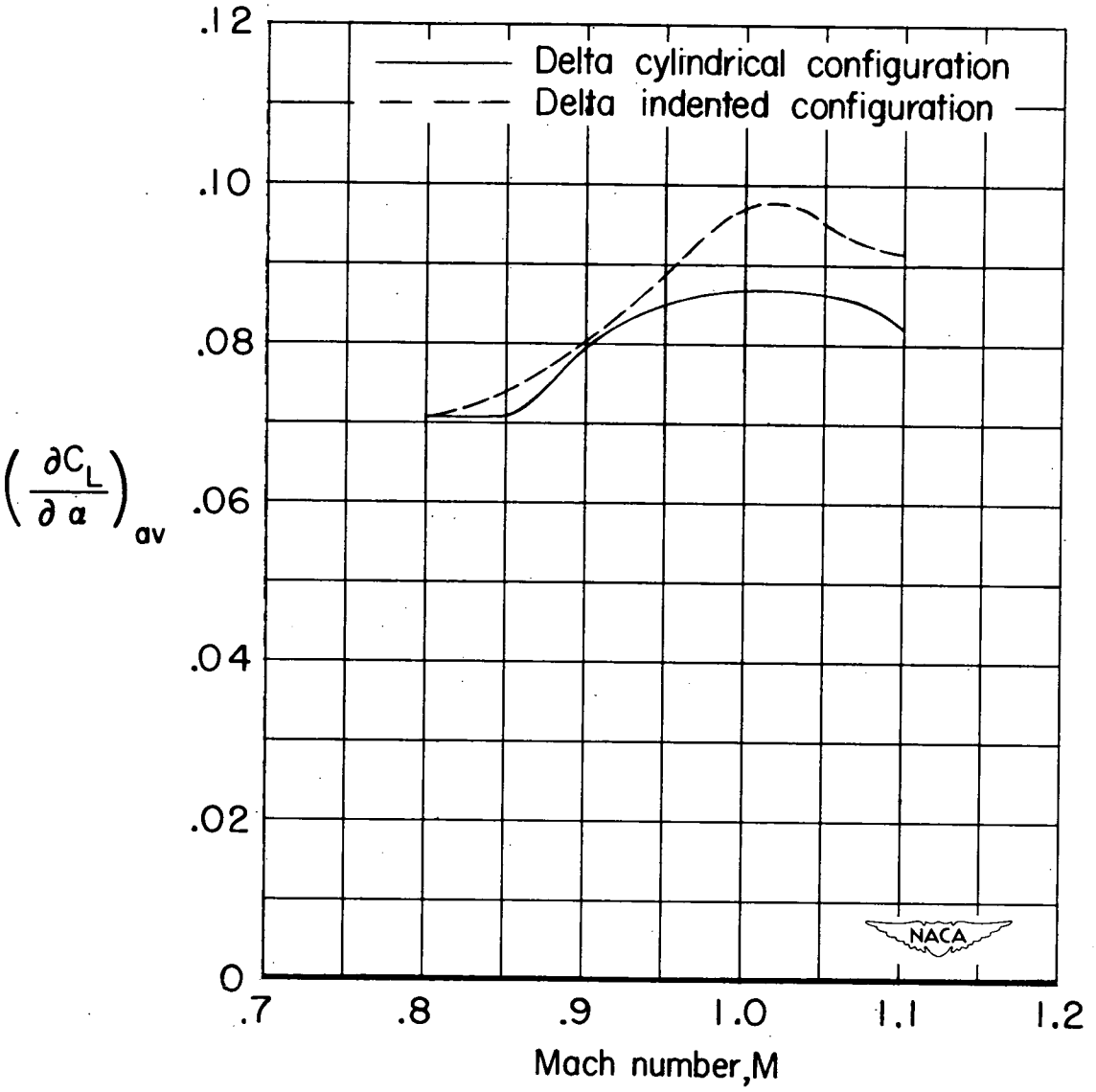

Figure 7.- Average lift-curve slope for the delta cylindrical and delta indented configurations.

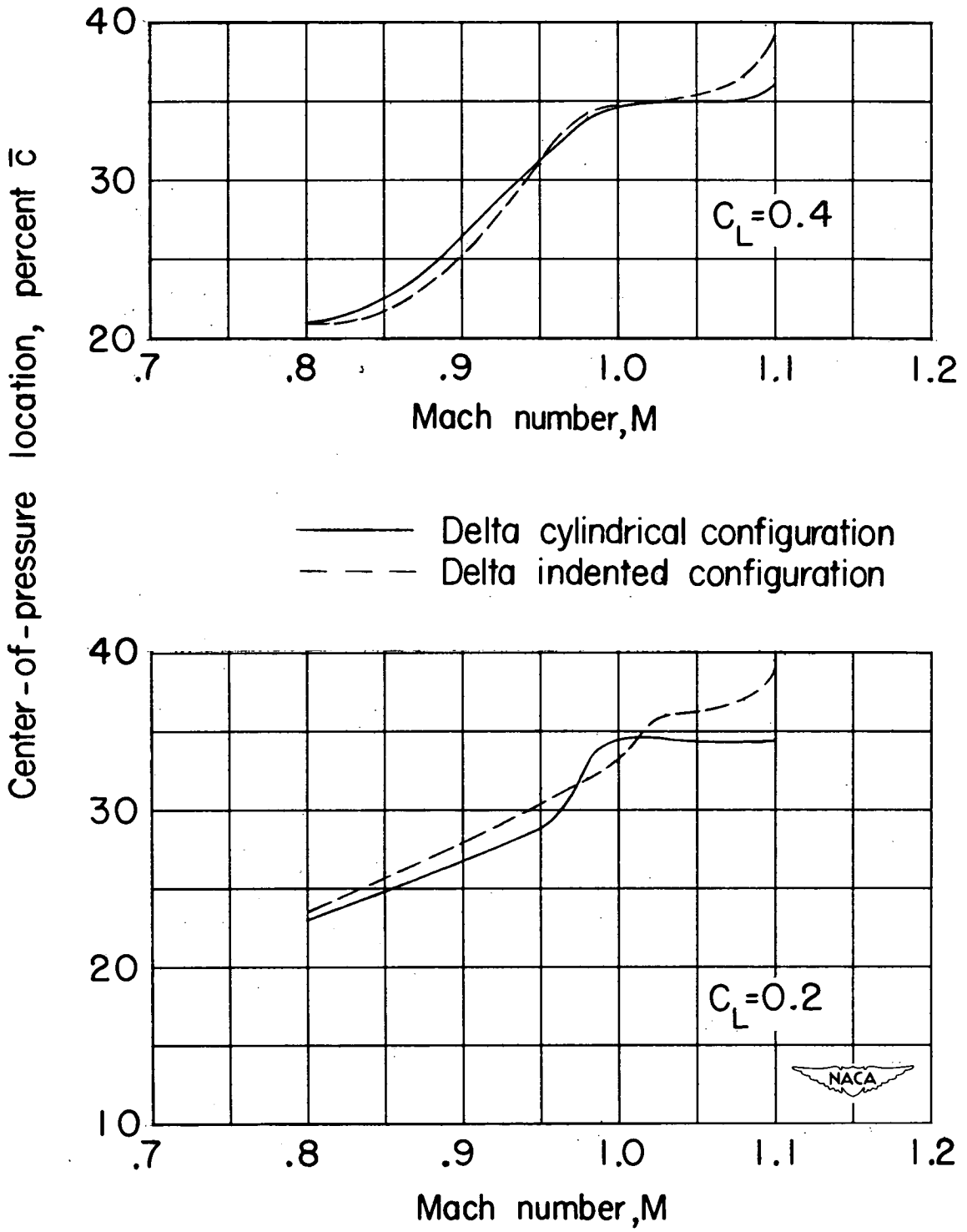

Figure 8.- Variation of the location of the center of pressure at lift coefficients of 0.2 and 0.4 for the delta cylindrical and delta indented configurations.

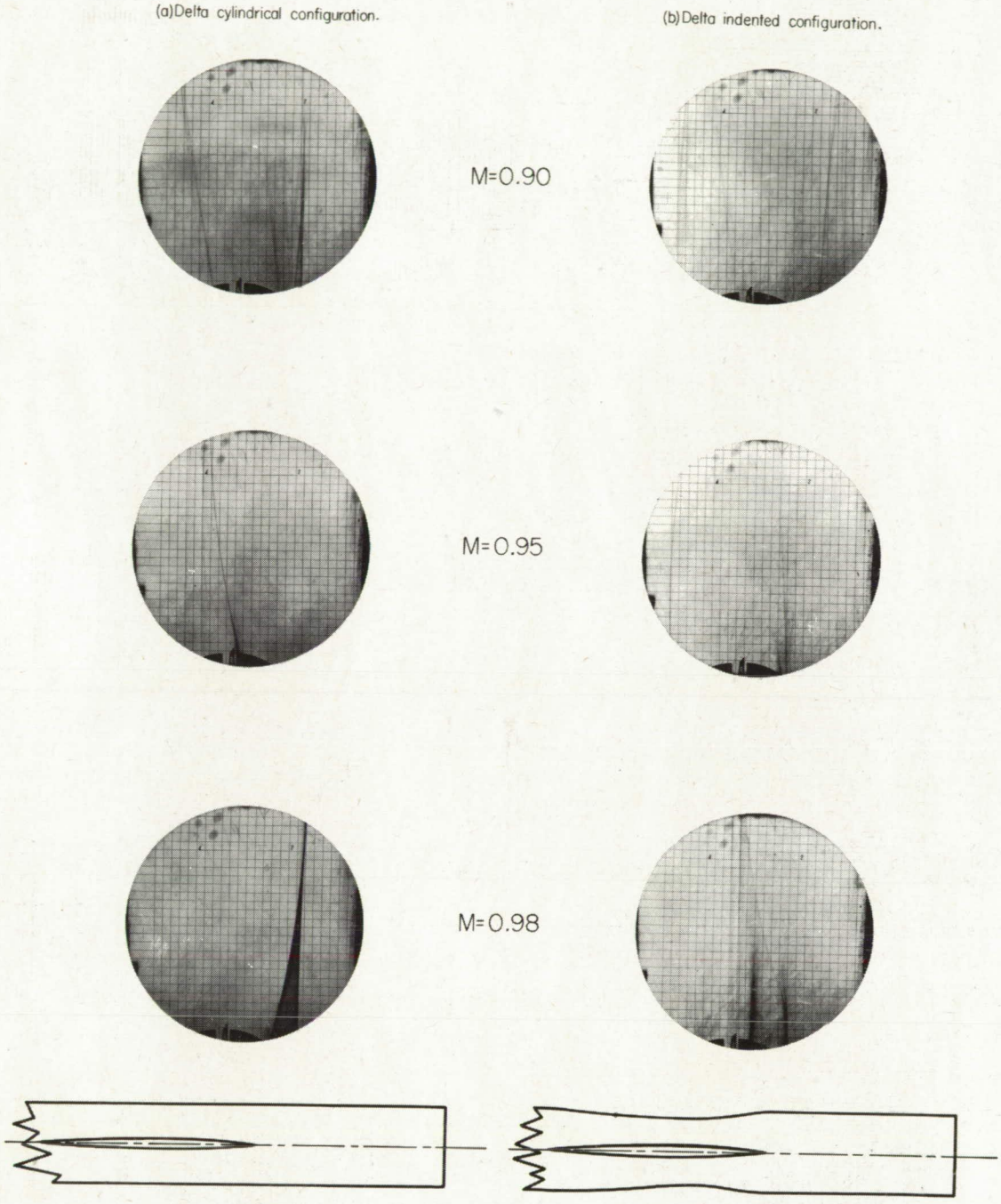

Figure 9.- Flow phenomena at an angle of attack of 0° for the delta cylindrical and delta indented configurations.

L-79273

(a) Delta cylindrical configuration.

(b) Delta indented configuration.

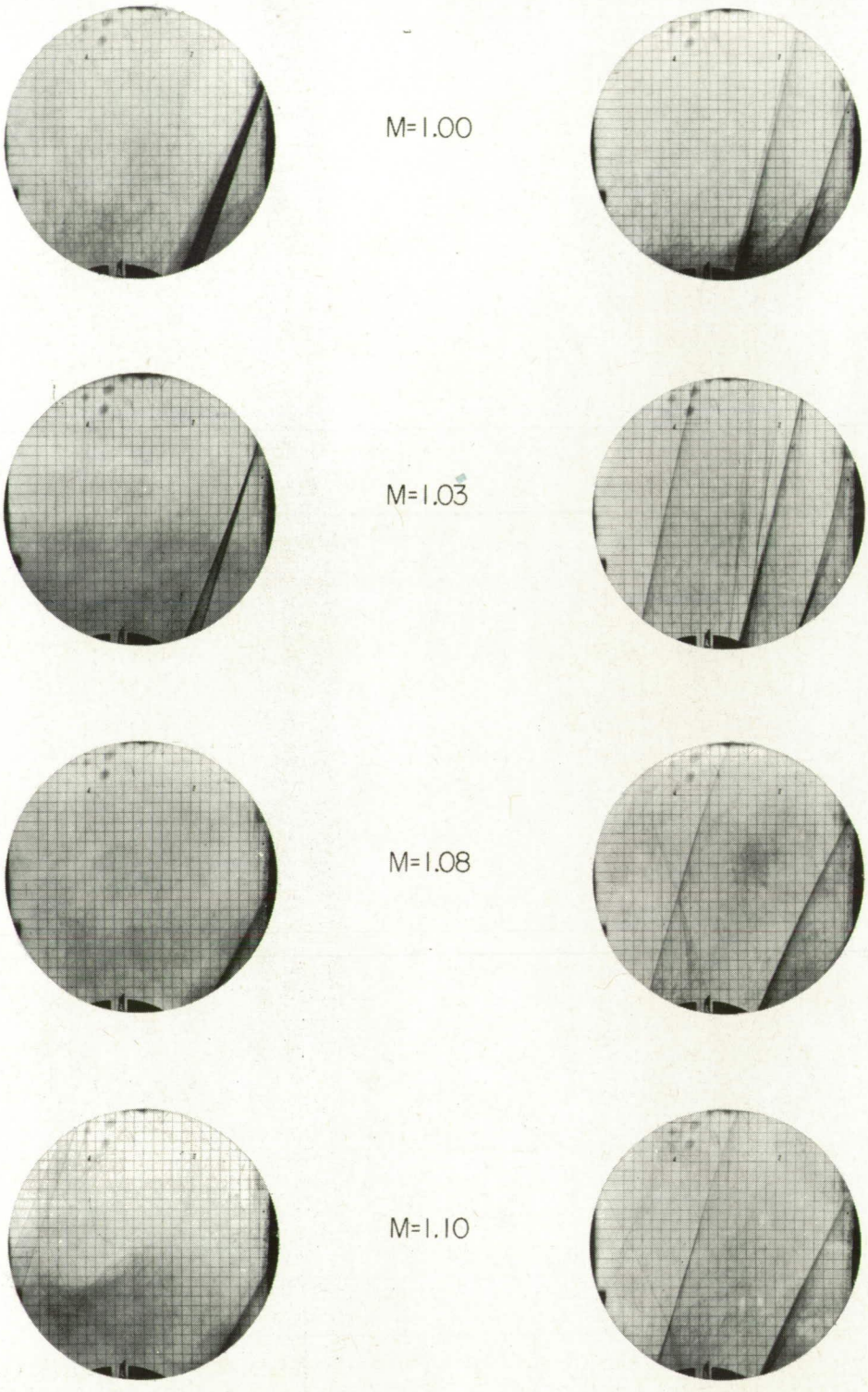

Figure 9.- Concluded.

NACA L-79274

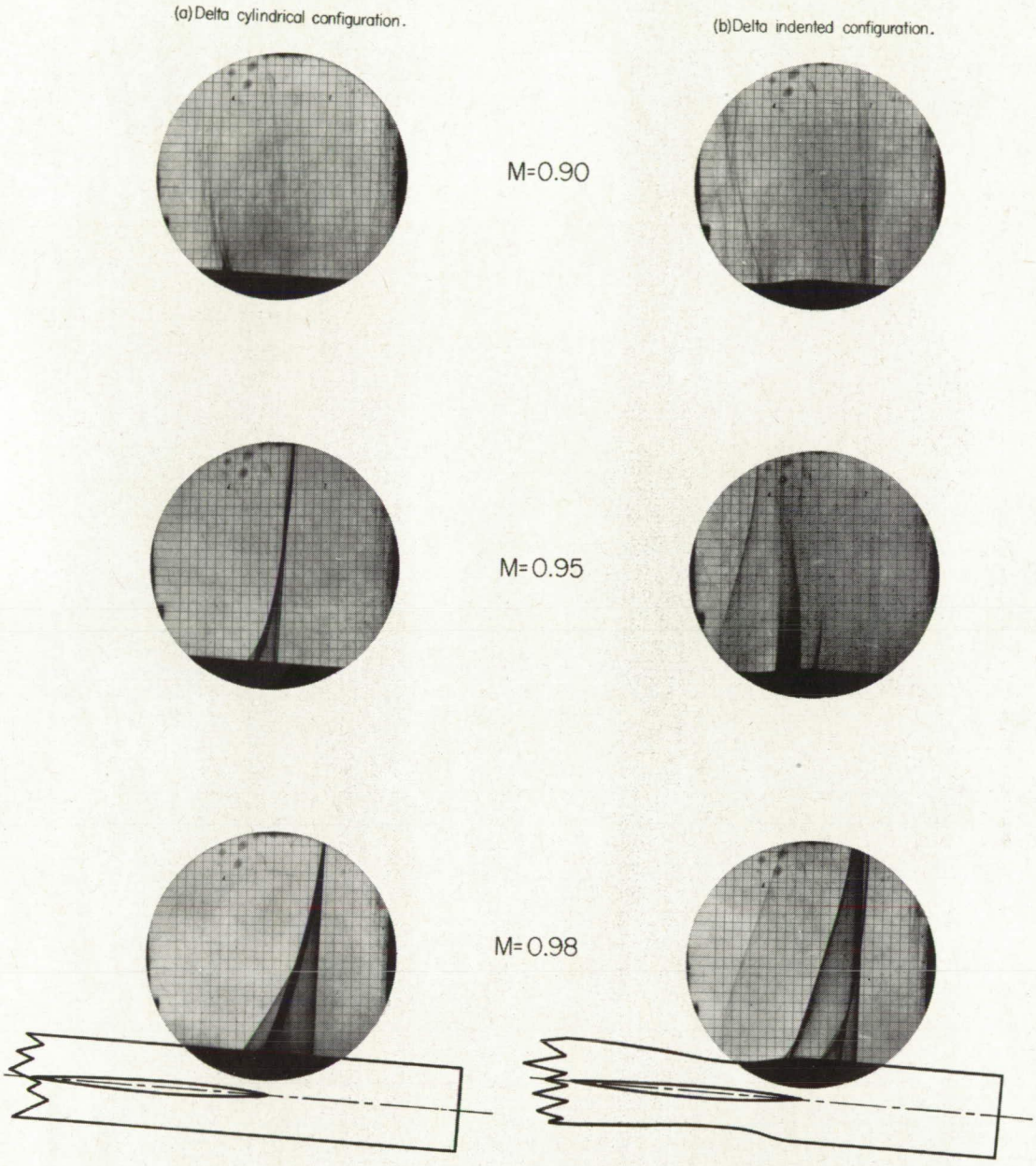

Figure 10.- Flow phenomena at an angle of attack of 4° for the delta cylindrical and delta indented configurations. NACA L-79275

(a) Delta cylindrical configuration.

(b) Delta indented configuration.

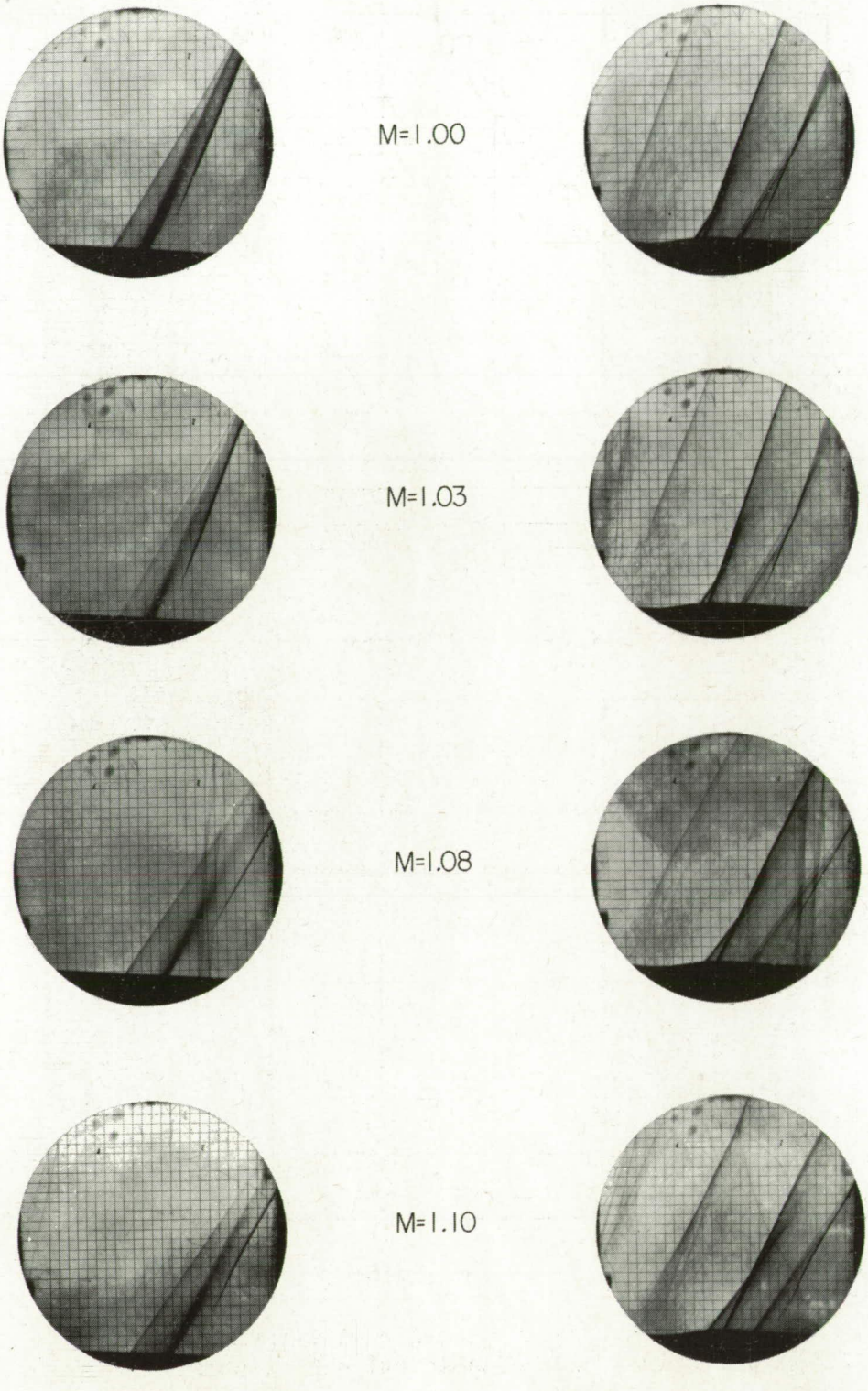

Figure 10.- Concluded.

NACA L-79276

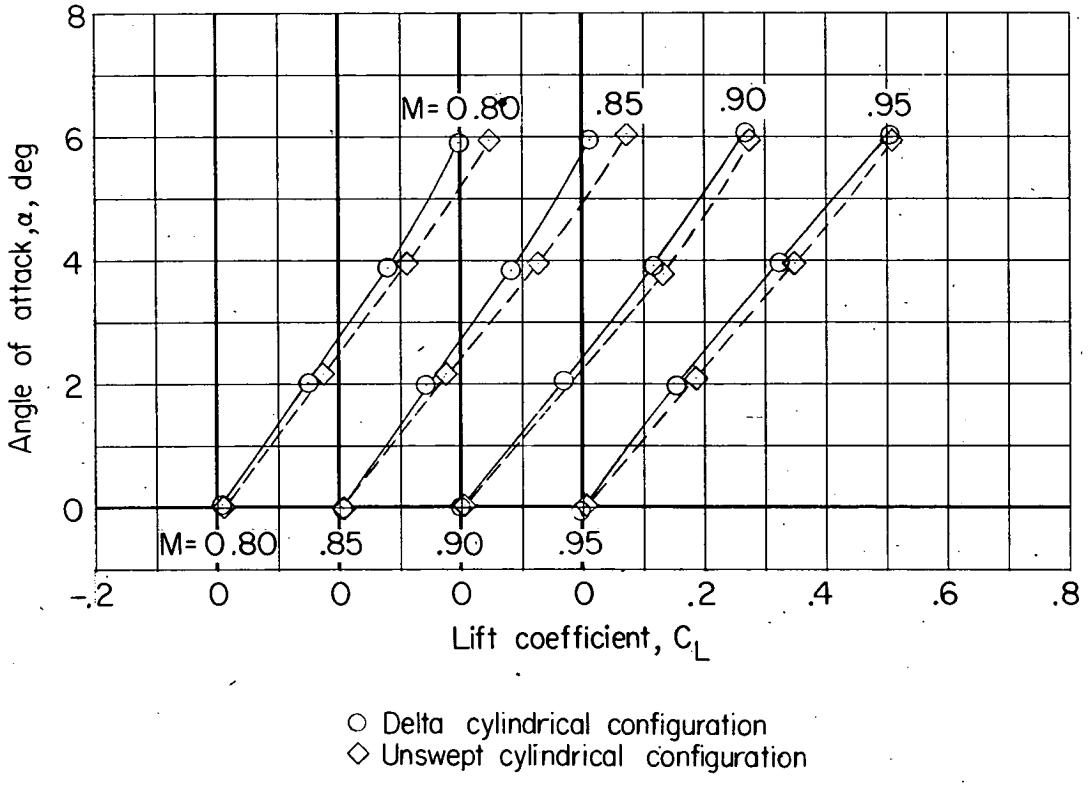

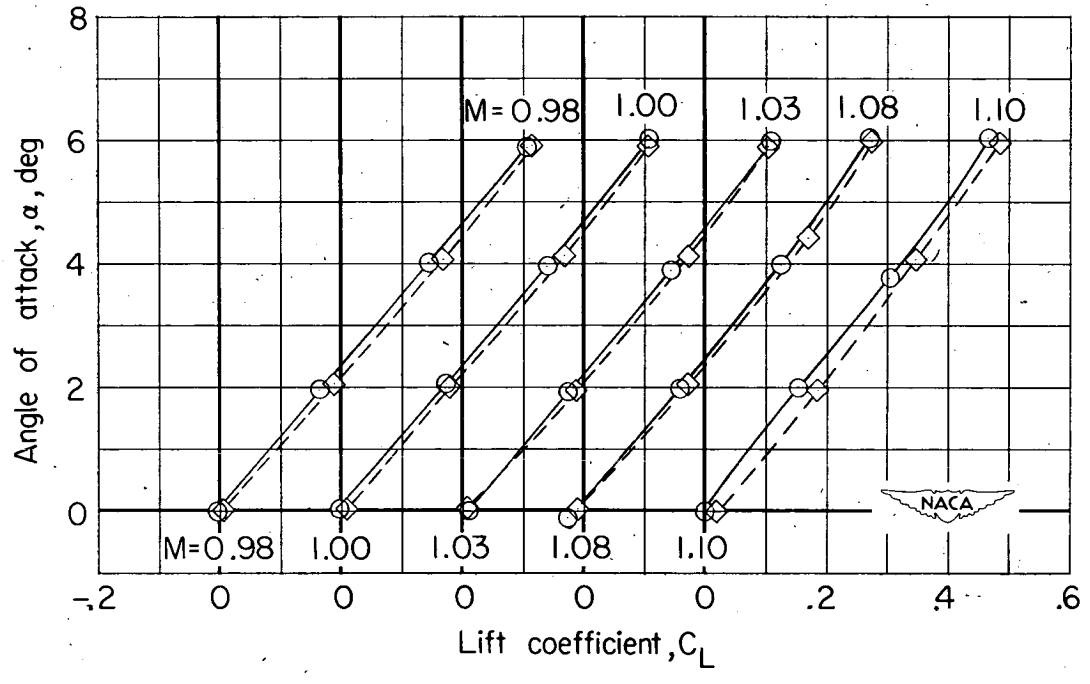

(a) α against C_L.

Figure 11.- Basic aerodynamic characteristics for the delta cylindrical and unswept cylindrical configurations.

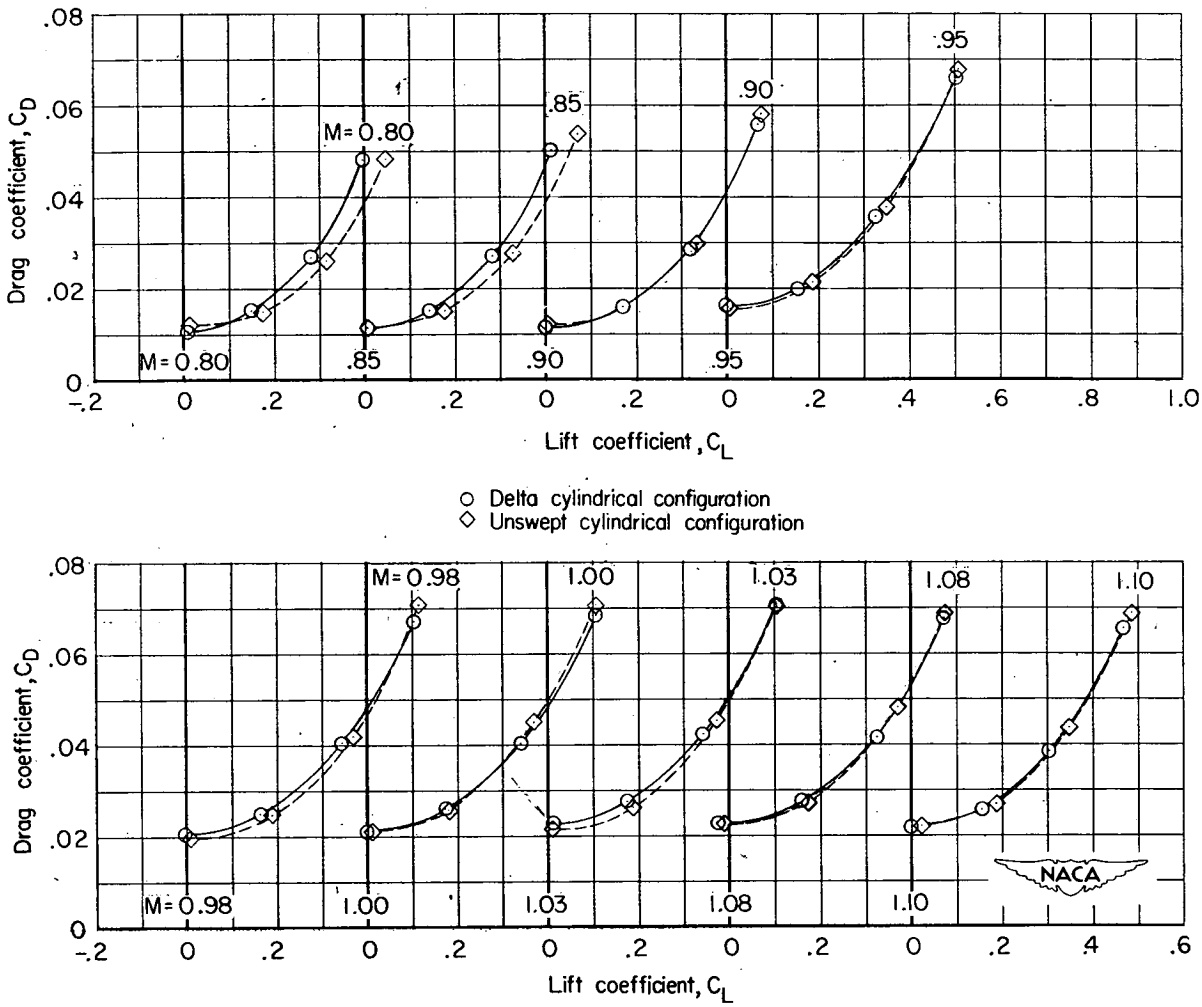

(b) C_D against C_L.

Figure 11.- Continued.

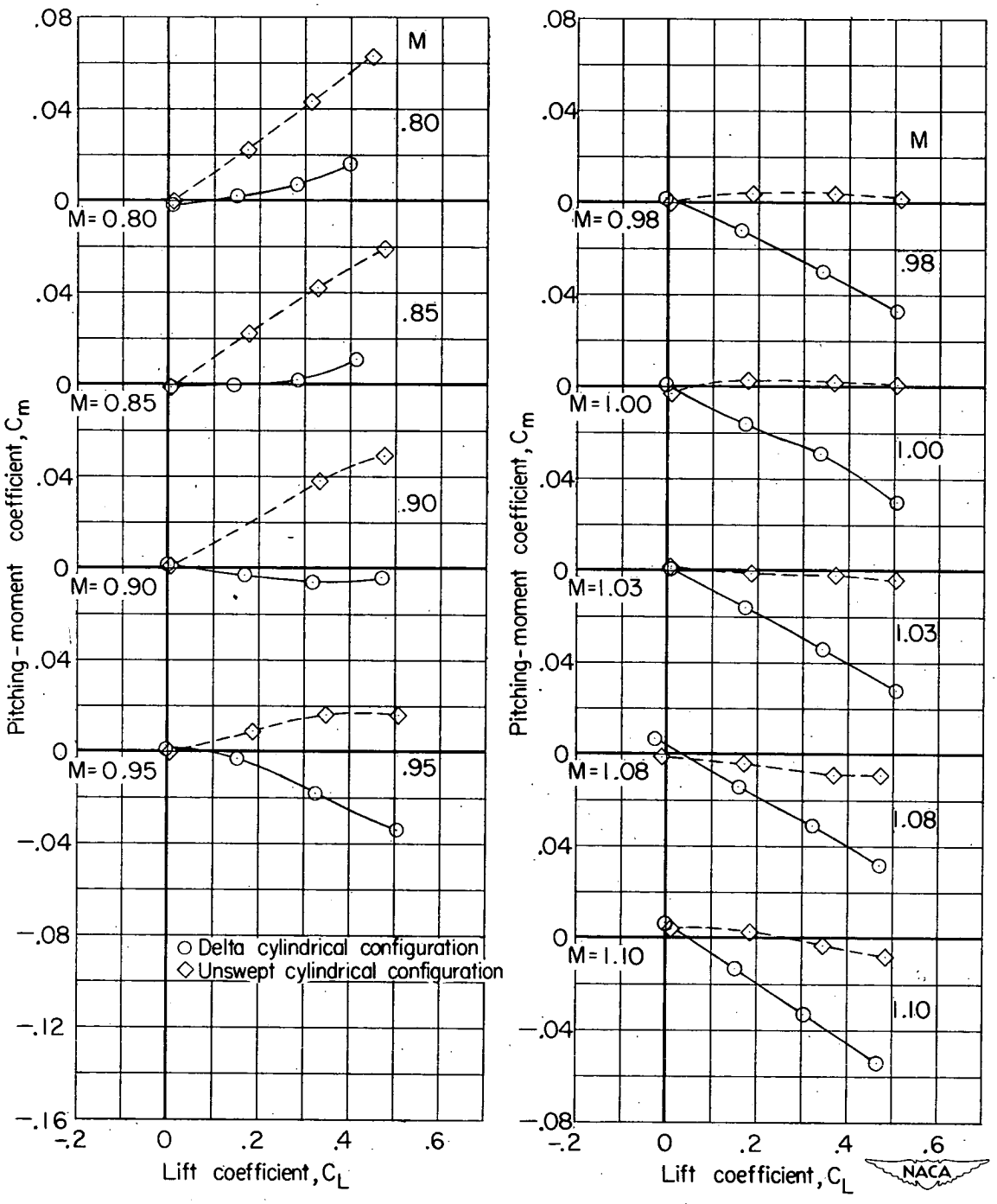

(c) C_m against C_L.

Figure 11.- Concluded.

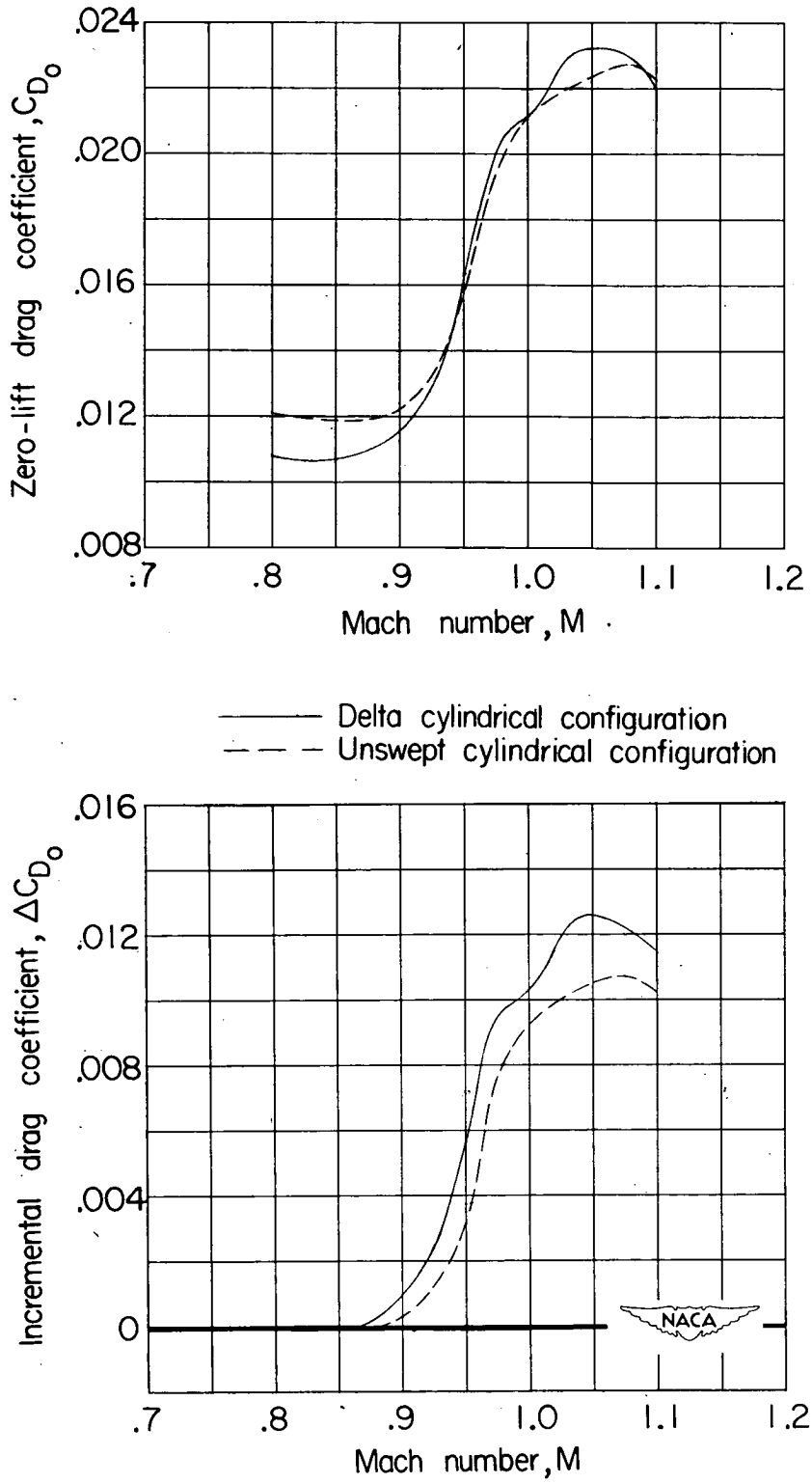

Figure 12.- Zero-lift drag characteristics for the delta cylindrical and unswept cylindrical configuration. (Data from ref. 1.)

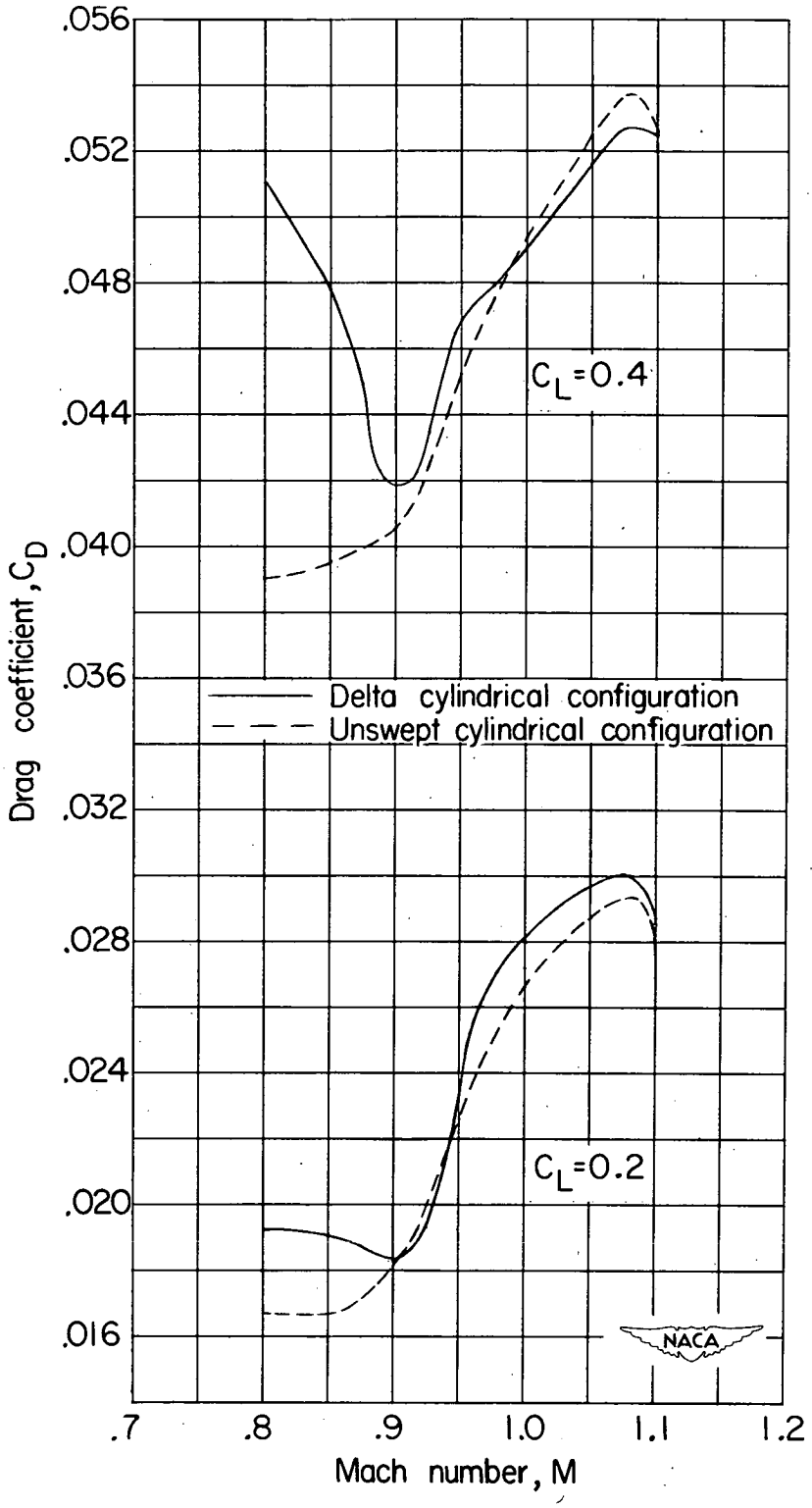

Figure 13.- Drag characteristics at lift coefficients of 0.2 and 0.4 for the delta cylindrical and unswept cylindrical configurations.

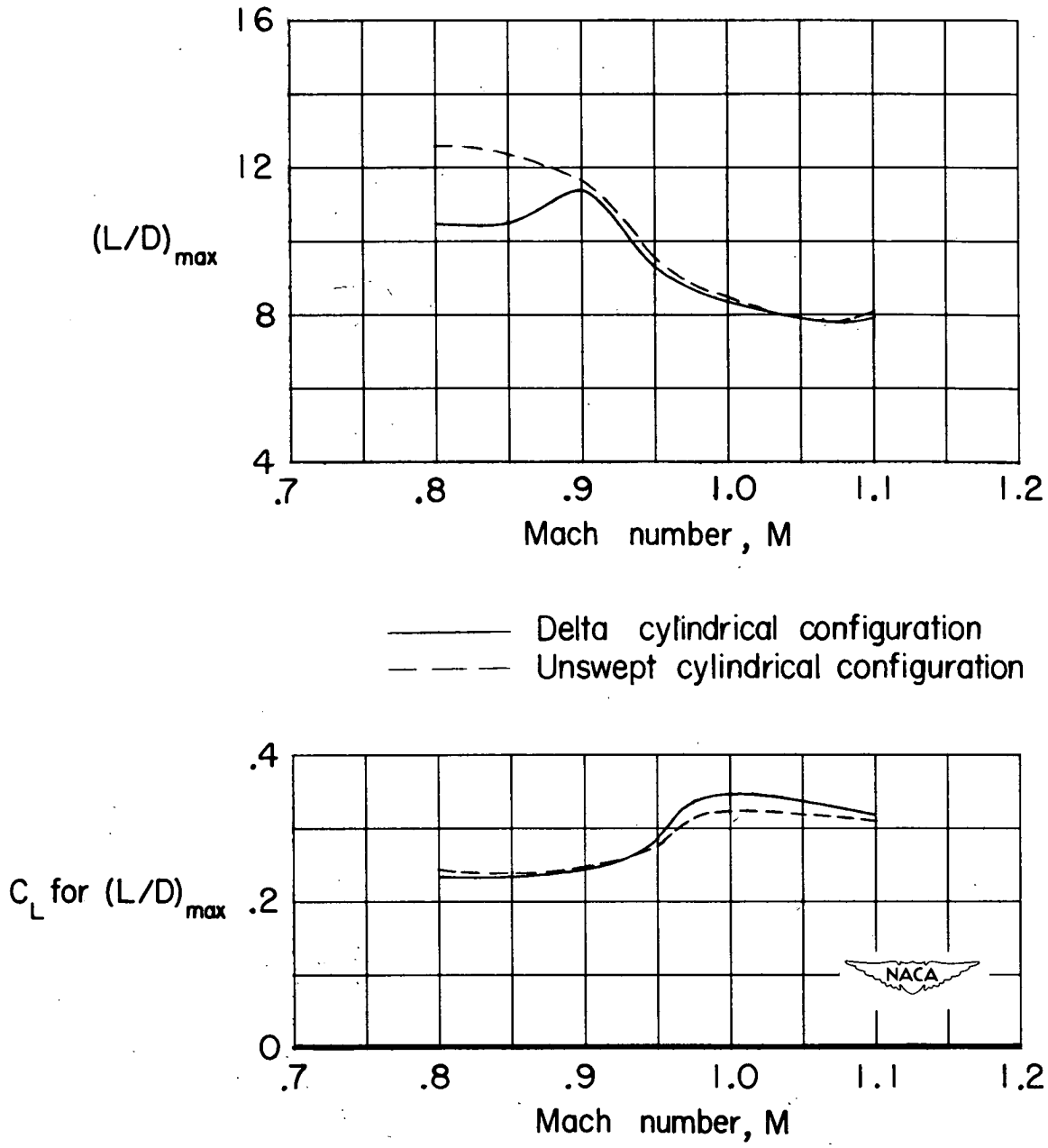

Figure 14.- Maximum lift-drag ratio and lift coefficients for maximum lift-drag ratio for the delta cylindrical and unswept cylindrical configurations.

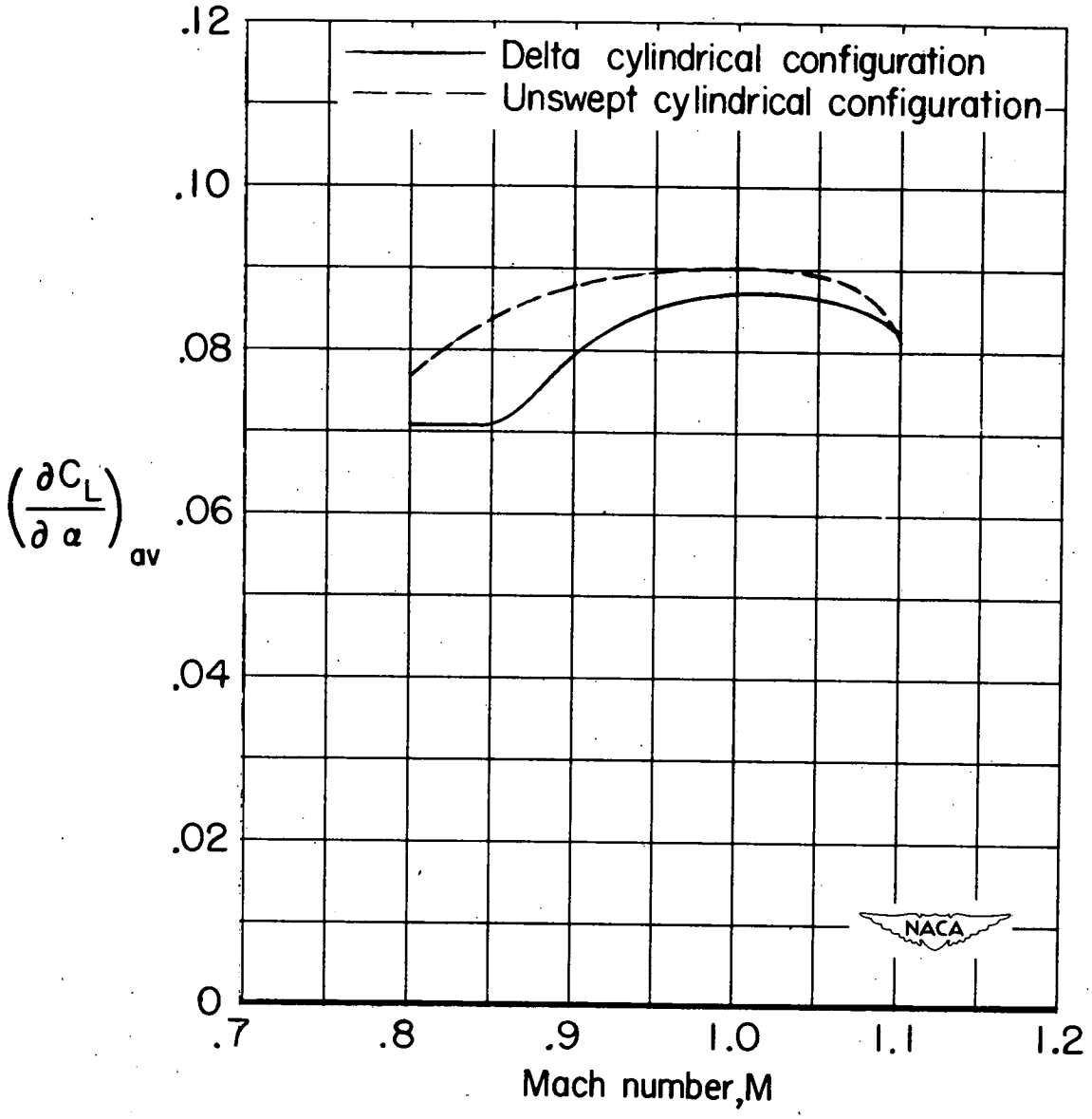

Figure 15.- Average lift-curve slope for the delta cylindrical and unswept cylindrical configurations.

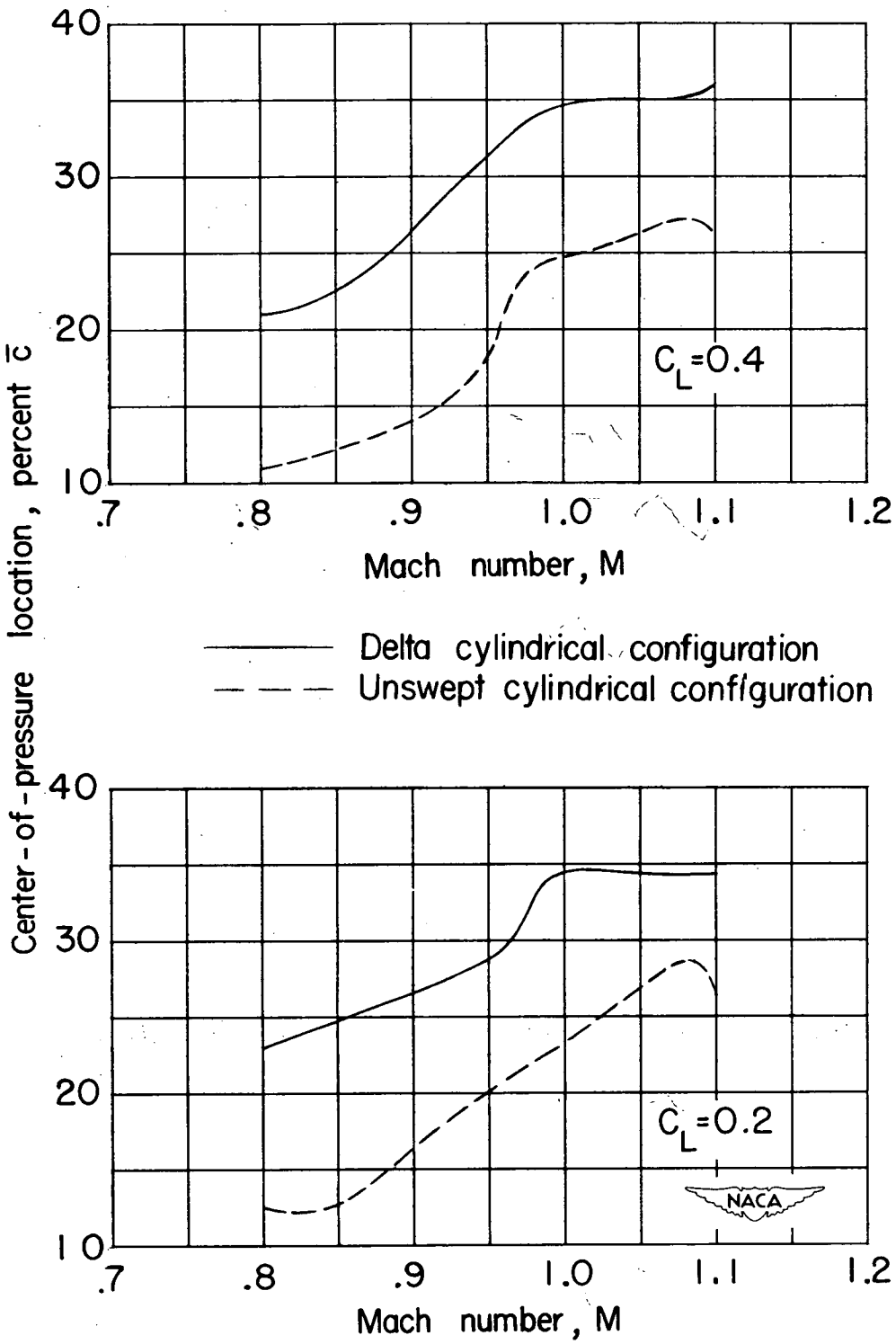

Figure 16.- Location of the center of pressure at lift coefficients of 0.2 and 0.4 for the delta cylindrical and unswept cylindrical configurations.

NACA-Langley - 8-13-53 - 325